Telemetry system driven by radiation power for use in gravitational wave detectors

Yi Zhao, Chunnong Zhao, Li Ju, Michael Small, and David G. Blair

Additional information on Rev. Sci. Instrum.

Telemetry system driven by radiation power for use in gravitational wave detectors

Yi Zhao
Hong Kong Polytechnic University, Kowloon, Hong Kong, China and School of Physics,
The University of Western Australia, 35 Stirling Highway, Nedlands, WA 6009, Australia

Chunnong Zhao[a)] and Li Ju
School of Physics, The University of Western Australia, 35 Stirling Highway, Nedlands, WA 6009, Australia

Michael Small
Hong Kong Polytechnic University, Kowloon, Hong Kong, China

David G. Blair
School of Physics, The University of Western Australia, 35 Stirling Highway, Nedlands, WA 6009, Australia

To prevent electrical wiring from mechanically short circuiting in the high performance vibration isolators for gravitational wave detection, we designed a telemetry system. The system provides wireless signal transmission and radiation power supplies. A consideration of heat dissipation of in-vacuum electronic components is presented. The preliminary experiments demonstrated that the telemetry system is feasible. © *2005 American Institute of Physics.* [DOI: 10.1063/1.1994988]

I. INTRODUCTION

The laser interferometric gravitational wave detector aims to directly detect gravitational waves by measuring the relative arm length variation induced by gravitational waves. This is done by observing the relative phase change between two interfering laser beams of a Michelson interferometer. A network of laser interferometric gravitational wave detectors[1–6] have been taking data or are being commissioned with planned spectral strain sensitivity of $\sim 10^{-23}$ Hz$^{-1/2}$, or spectral displacement sensitivity of $\sim 10^{-19}$ m Hz$^{-1/2}$.

To reach such extremely high sensitivity, very good isolation against seismic noise is required. While this has been achieved by suspending each mirror (acting as test mass) at the end of a multistage pendulum, the large amplitude pendulum motions must be accurately controlled to bring the interferometer towards its optimal working configuration. Moreover, the whole system must be in a good vacuum in order to avoid perturbations of the interferometer signal by refractive index fluctuations of the residual gas.

One frequently used control system in the interferometric gravitational wave detectors is comprised of motion sensing by a shadow sensor and actuation by a system of coils and magnet.[7] The shadow sensor consists of a blade fixed to the test mass which cuts part of the light path between a light-emitting diode and photodiode. The blade position determines the photocurrent. The feedback control signal is derived from an analog circuit or digital embedded controller, which executes relative calculation, to either damp the motion or to position the isolator. It requires a large number of wires to transmit motion sensing signals and actuation sig-

nals between the isolator in vacuum and the controller in air. Especially for the control of the test mass, all these wires have to be deliberately wired through the vibration isolator stages to minimize the seismic coupling through the wires. However, resonant bar gravitational waves detectors showed that cable noise was a serious issue.[8] The resonant bar NIOBE developed a noncontacting readout system, which dramatically improved its noise performance.[9] The test mass position and orientation measurement system developed by the VIRGO group based on a charge coupled device (ccd) imaging system avoided wiring on the isolator and between the vacuum and the air for sensing.[10] The actuations still
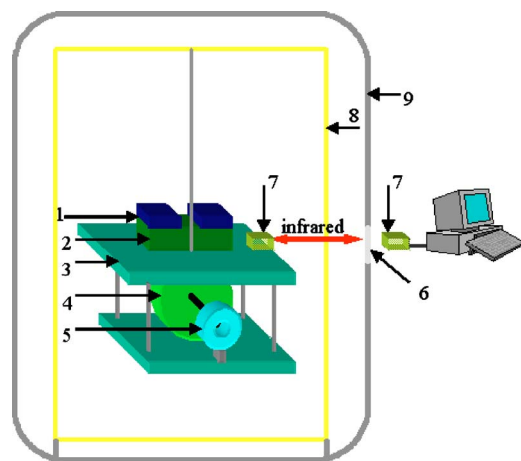

FIG. 1. (Color online) Schematic diagram of the telemetry system and two stage isolator: (1) photosilicon arrays; (2) the embedded system; (3) reference masses; (4) test masses; (5) shadow sensor and coil; (6) glass window; (7) emitting/receiving diodes; (8) frame; and (9) vacuum tank. Photosilicon arrays, shadow sensor and coil, and diodes are connected to the embedded system with wires. The embedded system is installed on reference masses. A set of diodes on reference masses inside the tank points to another set of diodes outside to execute signal transmission.

a)Author to whom correspondence should be addressed; electronic mail: zhao@physics.uwa.edu.au
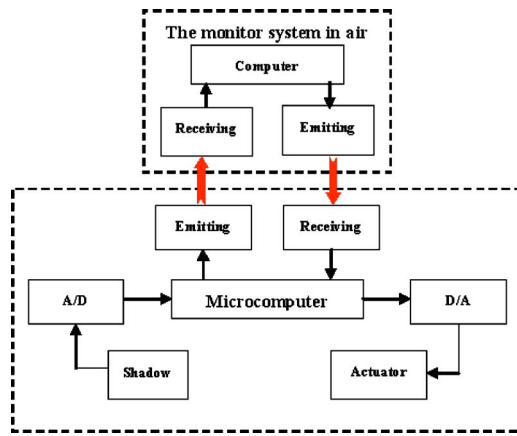
FIG. 2. (Color online) Schematic of the telemetry actuation system. The microcomputer of the embedded system administrates the actuator-shadow pairs. It sends the motion-sensing signal of the shadow sensor to the monitor system and receives the gain from it for the actuator. Red arrows indicate infrared signals.

required massive wiring through the isolator. It was proposed[11] that noncontacting infrared telemetry actuation system could be used to eliminate the seismic noise coupling from the wire. Here we present experimental results of telemetry actuation on two stage pendulums, which aims to replace all wires and realize truly wireless communication for the test mass control.

II. TELEMETRY SYSTEM

We used a two stage vibration isolator in a vacuum tank to test the telemetry system. A test mass is suspended from a reference mass platform which was suspended from a support frame. We used a shadow sensor on the test mass for sensing the motion and magnet/coil pair for actuation. Our system consists of two subsystems, the embedded system on the reference platform inside the vacuum tank, and the monitor system outside in air. In order to realize communication between the two subsystems over a relatively short distance, we adopt infrared with a wavelength of 850–900 nm to transfer all signals. Infrared is highly adapted to point-to-point communication over short distances. The telemetry system and the schematic of the two stage isolator are shown in Fig. 1.

The shadow sensor and the coil actuator are connected to the embedded controller with wires, which is mounted on the

reference mass platform. Two photosilicon arrays are also mounted on the reference mass stage to provide power (± 15 V) to the embedded system. The infrared transceiver of the embedded system points to that of the monitor system in air. The shadow sensor collects the one-dimension motion signals of test masses relative to the reference mass. The actuator (coil/magnet) with feedback keeps the test masses stable in that direction. The embedded system executes all the following tasks: analog to digital (A/D) conversion, computing, transmitting data of motion sensing and receiving gain signal though infrared diodes, and digital to analog (D/A) conversion. Figure 2 shows the schematic of the embedded system and monitor system.

There are two types of signal required to transmit between the two subsystems: sampled motion-sensing signal that is transmitted all the time, and the value of gain that is transmitted as required.

The procedure of the telemetry actuation system is as follows:

(1) The motion-sensing signal from the shadow sensor is amplified and passed to the A/D converter. We selected ADS7813 of Analog Devices as the A/D converter. Its internal high-speed clock simplifies data synchronization and matches our requirement on sampling speed.

(2) The microcomputer starts A/D conversion and saves digital data of the motion-sensing signal. Then the microcomputer executes the computation.

(3) Sampled data are transmitted to the monitor system outside through the infrared communication. The monitor system is connected to the serial interface of a computer. We adopt *LabView* to design the interface software, which reads and saves the data received and plots the waveform of motion-sensing signal in real time. Figure 3 displays the interface of this software monitoring the real-time position of test masses. We can also send the value of gain, which adjusts the amplitude of the feedback, to the embedded system inside through this interface software.

(4) According to the value of gain set by the embedded system or received remotely, the microcomputer obtains the feedback signal multiplied by the gain and writes it to the D/A converter. After filtering and amplification the signal is applied to the coil to control the test mass.
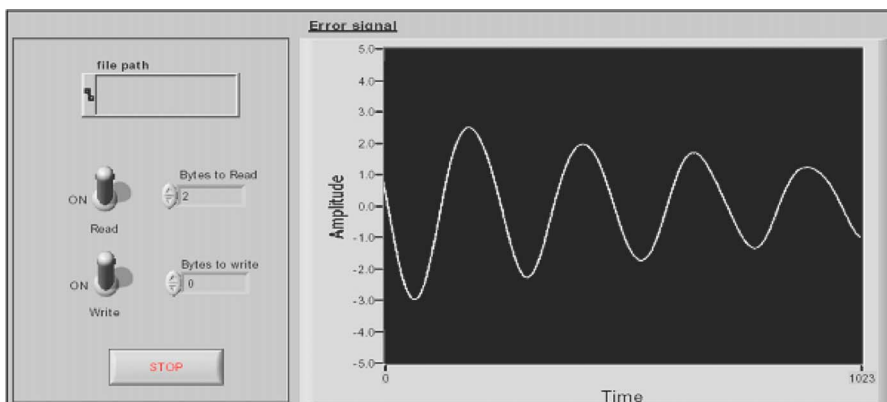

FIG. 3. Interface of the monitor software. The READ button is to enable the software to receive the data from the interface of RS 232. The WRITE button is to enable the software to transmit the gain, which can be modified in the small window besides it, to the embedded system. The large window is aimed to show the real-time waveform that of the movement of the test mass.
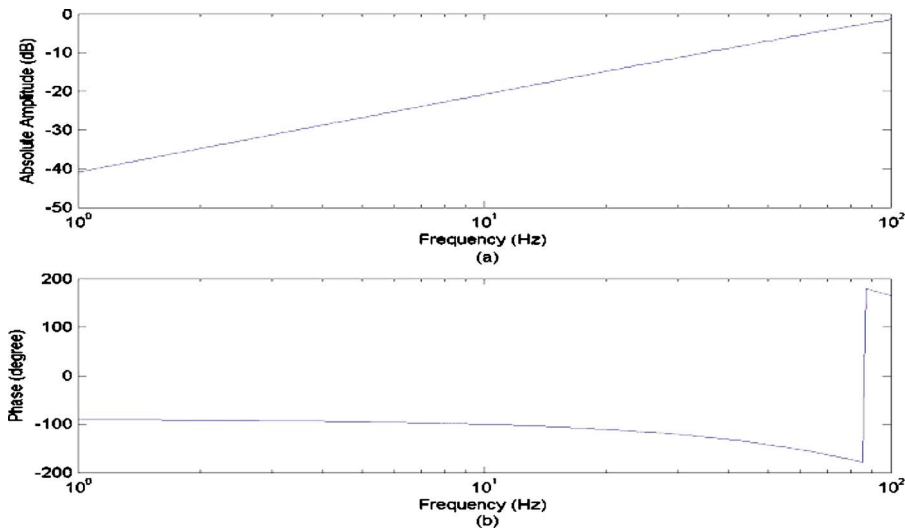
FIG. 4. Bode plots of the embedded system (A/D, D/A, and microcomputer). The phase delay increases with the signal frequency due to the time delay.

III. CONSIDERATION OF THERMAL RADIATION IN VACUUM

The vibration isolation system and test masses in gravitational wave detectors will operate in a vacuum. Thus the embedded system, including photosilicon arrays, must work inside a vacuum as well. In the vacuum the material dissipates heat to the outside through thermal conduction of the thin suspension wire and thermal radiation. Thus during operation the surface temperature of electronic components of the embedded system and photosilicon arrays may become a serious issue.

We first consider thermal radiation only. According to the Stefan–Boltzmann law, the net radiative heat transfer rate is given by

$$P = e\sigma A(T_s^4 - T_a^4), \tag{1}$$

where e is the emissivity of the object; σ is the Stefan's constant, $\sigma = 5.6703 \times 10^{-8}$ W m^{-2} K^{-4}; A is the radiating area of the object; and T_s is the absolute temperature of the object; and T_a is the absolute temperature of environment. Below, we roughly estimate the temperature of the microcontroller and photosilicon arrays when operating in a vacuum, using some typical parameters.

The power dissipation of the microcontroller P_{con} is 1.5 W; its surface area is 51.5×13.7 mm^2. Supposing P_r is the radiative heat-transfer rate, the temperature of the microcontroller T_{con} is calculated by[12]

$$T_{con}^4 = T_a^4 + \frac{P_{con}}{e\sigma A}. \tag{2}$$

Given e is equal to 0.90, and the environment temperature is 300 K (27 ° C), T_{con} is about 472 K (195 ° C). This temperature is far higher than the temperature range of the microcontroller (0–70 ° C). The suspension wire may dissipate part of the heat to the outside through thermal conduction. If the electronic components can dissipate heat to the mechanical suspension structures, especially for the all-metal structures, that will ease the heating problem. The outgassing of chips is another issue in the vacuum because they are not designed to be used in the vacuum. To solve this problem, we propose to vacuum seal all electronics inside a metal box. There is direct thermal contact between the electronic component surface and the inner surface of the box, which increases the efficiency of heat transfer for the embedded system.

For instance, for a box of $100*100*50$ mm^3 in size, to dissipate 4.2 W power which is required by the microcontroller and one dimensional control, the box surface temperature will only rise to 318 K or 45 ° C, with a similar temperature rise for the electronic components. The component temperature rise will not be a problem. The component outgassing should not be an issue either because of the vacuum seal.

Wang et al.[11] have shown that by using a fiber-coupled infrared diode laser to deliver light to the crystalline silicon cell, it is feasible to provide radiation power to the telemetry system. An interlocking heat sink could be used to provide an efficient cooling path to radiate heat from photosilicon arrays to copper conduction plates mounted on the vacuum tank.

IV. EXPERIMENTAL RESULTS

A prototype telemetry system was built, as shown in Fig. 1, to demonstrate the feasibility. The system was powered by two photosilicon arrays of ±15 V illuminated by two Halogen lights through windows. The vacuum tank was pumped down to $\sim 10^{-2}$ Torr by a mechanical pump. No special heat dissipation was implemented for the electronic components and photosilicon arrays at this stage. To prevent overheating the system was turned on for only ~ 5 min each time to obtain data and then turned off for cooling down. We first measured the time delay of the microcontroller using its internal clock as a time base. The time delay was ~ 1.67 ms that included A/D converter sampling, computing, and sending the signal to the D/A converter. This time delay corresponded to an actual sampling rate of ~ 600 samples/s of the system.

Using the SRS780 spectrum analyzer we measured the transfer function of the embedded system including A/D, D/A, and microcontroller. The plots are presented in Fig. 4. The analog circuits in the sensors and actuators are much
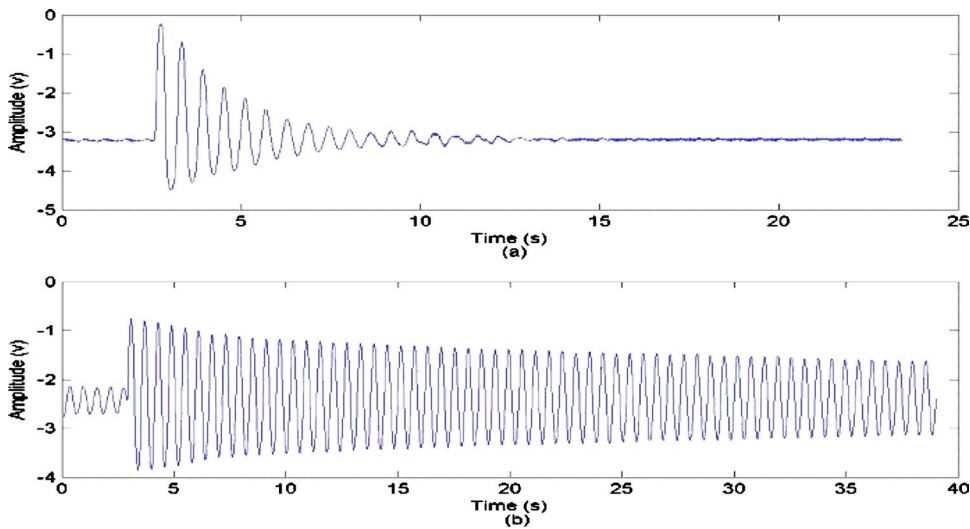
FIG. 5. (a) The ring down curve of the test masses damped by the embedded system and (b) the ring down curve of test masses without damping.

faster than the microcontroller and will not affect performance of the control loop. Their transfer functions are not included in the plots.

There was a phase delay of 45° at ~45 Hz. If we set the unity gain frequency of the control system to 45 Hz by tuning the loop gain there will be a 45° phase margin to keep the system stable. The control band width of 45Hz is also sufficient for the local control of the isolator.

The telemetry system was configured to apply velocity damping to the pendulum. Through the interface shown in Fig. 3 we can remotely change the damping gain. Figure 5 shows the pendulum ring down curve measured with (gain >1) and without (gain=0) damping. It is obvious from Fig. 5 that the test masses motion was damped effectively with damping on.

This prototype telemetry system demonstrated the feasibility of using infrared wireless communication and radiation power supplies to avoid noise coupling through wiring in advanced vibration isolators for gravitational wave detection. The proposed heat dissipation design will overcome the overheating of the electronic components and photosilicon cells in vacuum. Using an infrared diode laser as the light source for the photosilicon cells will increase the power efficiency and reduce the heat dissipation requirements for the photosilicon cells.

In our experiments the telemetry system controls the test masses in one dimension. It is feasible to extend the current system to control several degrees of freedom almost simultaneously. For example, we can add a four-channel multiplexer, whose output and inputs are connected to the A/D chip and four shadow sensors, respectively. The microcontroller of the embedded system will operate the multiplexer to selectively sample one shadow sensor at a time. For the DAC outputs, we can add a four-channel demultiplexer with sample hold outputs, which direct the D/A converter's output

to each of four actuators. Note that we have already saved adequate port pins in the current circuit, which can be used to operate these two chips. The embedded system will sample each shadow sensor through the multiplexer and output the feedback signal to the corresponding actuator by operating the demultiplexer in a coordinated way. It is true that the multichannel controls will share the same bandwidth of the controller. For a four control channel system described above, the control bandwidth of each channel will be close to 10 Hz which is enough to control the test mass with normal mode frequencies of ~1 Hz. Generally, four control channels are enough to control the test mass's four degrees of freedom (pitch, yaw, position, and side). If higher control bandwidth or more control channels are required we may consider more powerful controller or alternative configurations.

ACKNOWLEDGMENTS

[1] B. Abbott *et al.*, Nucl. Instrum. Methods Phys. Res. A **517**, 154 (2004).
[2] D. Sigg, Class. Quantum Grav. **21**, S409 (2004).
[3] F. Acernese *et al.*, Class. Quantum Grav. **21**, S395 (2004).
[4] B. Willke *et al.*, Class. Quantum Grav. **21**, S417 (2004).
[5] R. Takahashi *et al.*, Class. Quantum Grav. **21**, S403 (2004).
[6] M. Ando *et al.*, Phys. Rev. Lett. **86**, 3950 (2001).
[7] D. Shoemaker, R. Schilling, L. Schnupp, W. Winkler, K. Maischberger, and A. Rudiger, Phys. Rev. D **38**, 423 (1987).
[8] P. Vietch, PhD thesis, University of Western Australia, 1986.
[9] D. G. Blair *et al.*, Phys. Rev. Lett. **74**, 1908 (1995).
[10] F. Acernese *et al.*, Astropart. Phys. **20**, 617 (2004).
[11] X. Wang *et al.*, Class. Quantum Grav. **21**, S1023 (2004).
[12] Phillips Semiconductors, Data Sheet of 80C51 8-bit Flash microcontroller family 35, 2002.